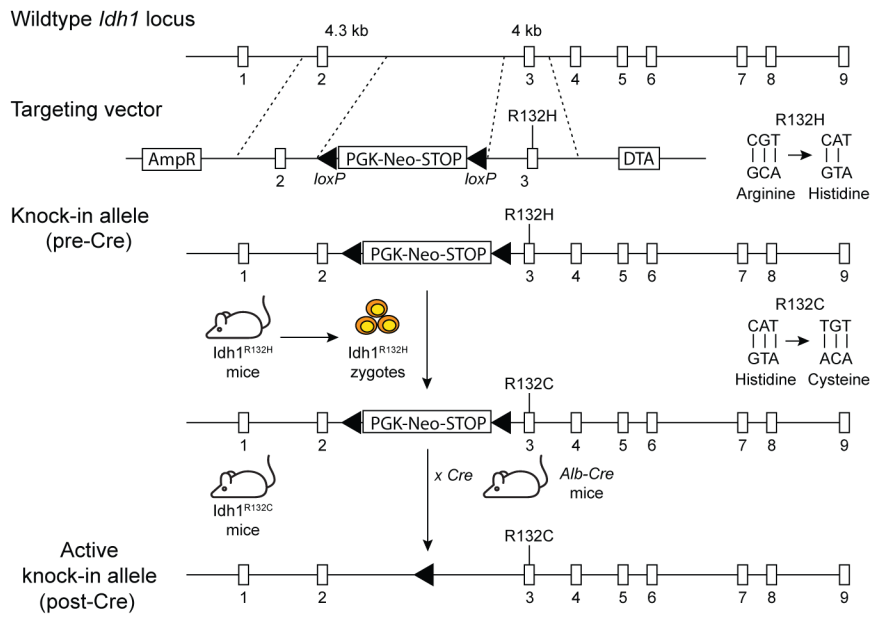
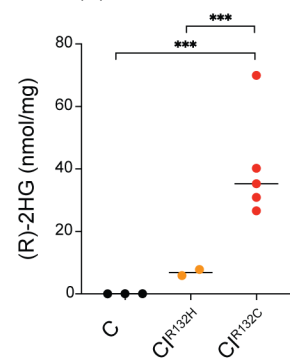


A

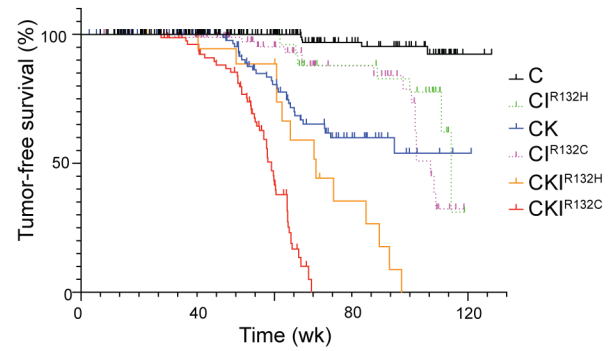


B

(R)-2HG in mouse liver

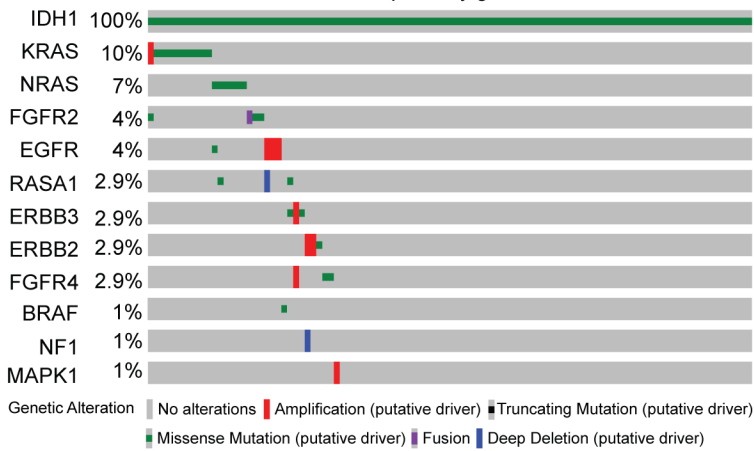


D

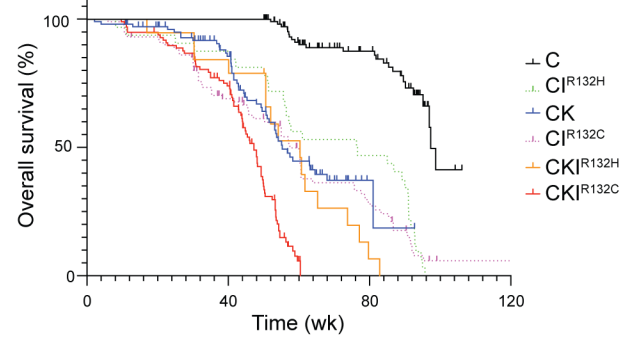


C

Concurrent activating mutations in RTK-RAS-MEK pathway genes in MIDH1 ICC



E



F

Sites of metastatic dissemination of ICC arising in the CKI^{R132C} GEM model

Mouse ID	Metastatic spread ^a						
	Kidney	Lung	Pancreas	Lymph node	Stomach	Peritoneum	Intestine
2275	✓	✓	✓	✓		✓	
3298			✓	✓		✓	
3955		✓		✓			
3959		✓		✓			
3961		✓					
4071		✓		✓			
4100		✓		✓			
4255		✓	✓	✓	✓	✓	
4377		✓		✓			
4411	✓		✓				✓
4609		✓					

*^a: All metastatic lesions showed ICC histology.

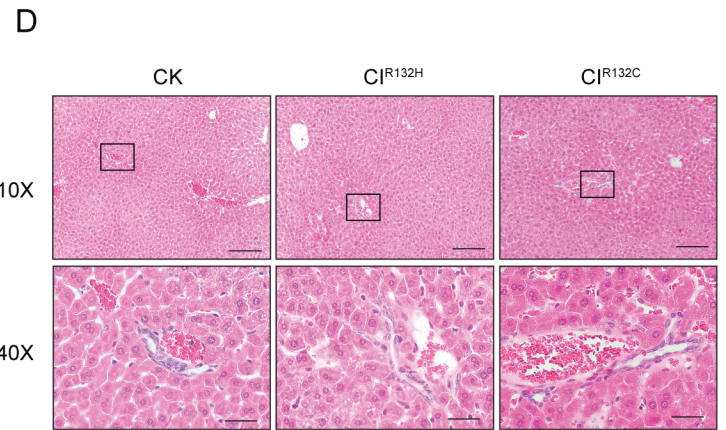
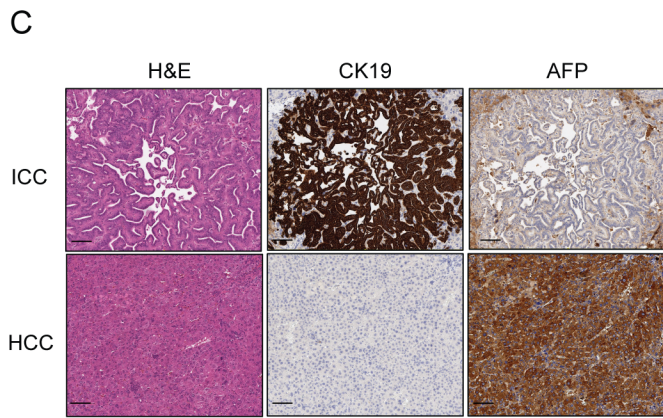
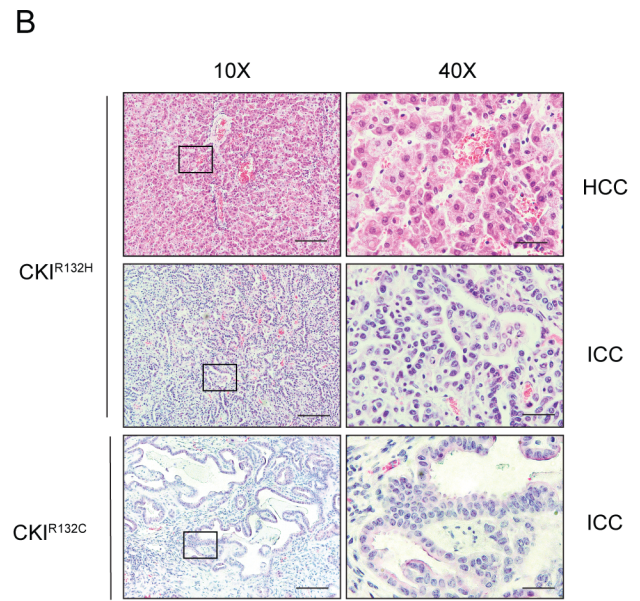
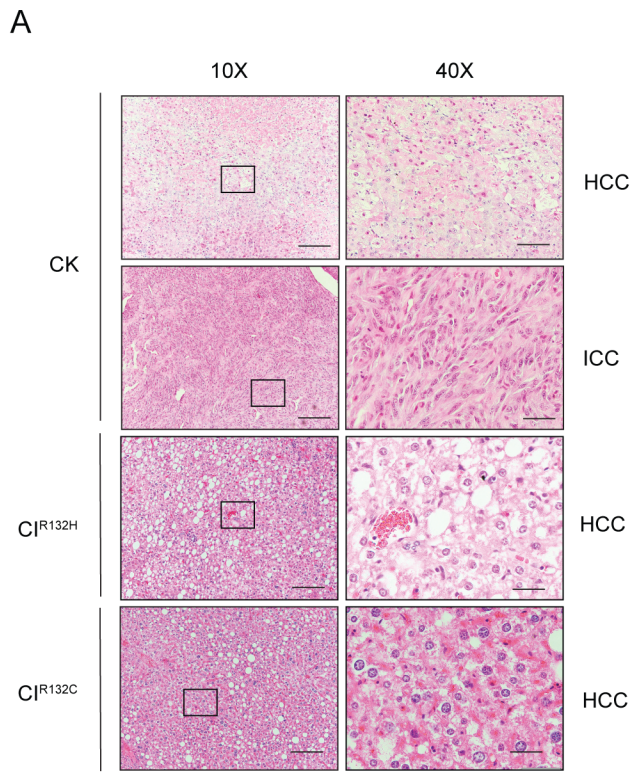
G

Tumor Incidence, Latency, and Histological Phenotype

Genotype	No. of mice with tumor	Tumor-specific median survival (weeks)	Metastasis (%)	Histology	
				% ICC [†] Major [‡] Any	% HCC [†] Major [‡] Any
Alb-Cre; Kras ^{G12D}	29	undefined	0	6.9 [†] (10.3) [‡]	93.1 [†] (100) [‡]
Alb-Cre; Idh1 ^{R132H}	6	95.7	0	0 [†] (0) [‡]	100 [†] (100) [‡]
Alb-Cre; Idh1 ^{R132C}	16	90.4	0	0 [†] (0) [‡]	100 [†] (100) [‡]
Alb-Cre; Kras ^{G12D} ; Idh1 ^{R132H}	13	60.2	0	7.7 [†] (23.1) [‡]	92.3 [†] (100) [‡]
Alb-Cre; Kras ^{G12D} ; Idh1 ^{R132C}	54	47.6	20.4	68.5 [†] (92.6) [‡]	31.5 [†] (55.6) [‡]

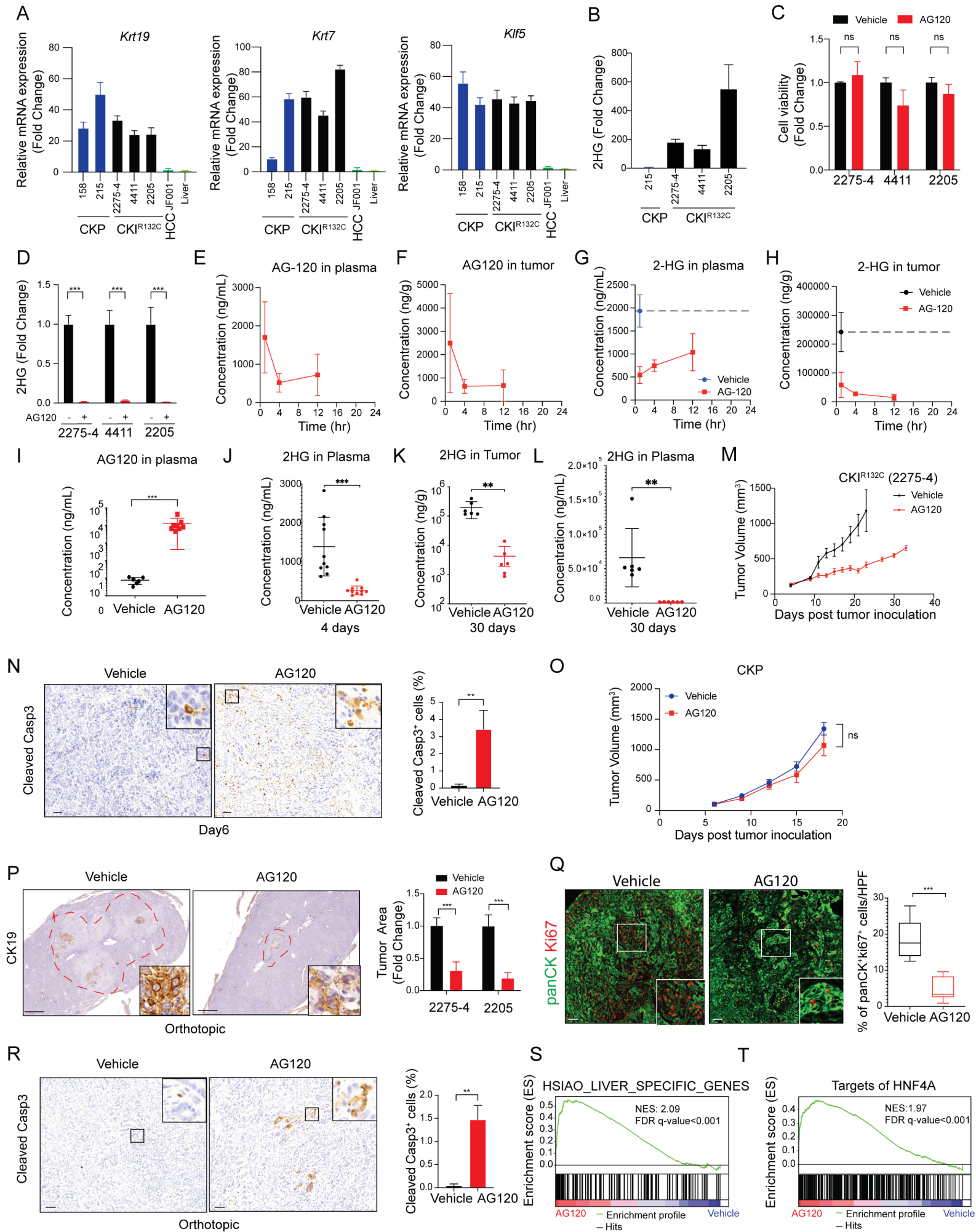
[†]: Percentage of mice in which the particular histology predominates.[‡]: Percentage of mice in which the particular histology is present in any proportion.

Supplementary Figure S1. Selective induction of murine ICC by the high (R)-2HG-producing *Idh1*^{R132C} allele (A) Schematic depicting the endogenous *Idh1* locus, the *Idh1*^{R132H} targeting vector and generation of the Lox-Stop-Lox (LSL) knock-in strains (see Methods). The *LSL-Idh1*^{R132C} allele was generated by CRISPR engineering of *LSL-Idh1*^{R132H} zygotes. Numbers below boxes indicate exons; lines represent introns. Cre-recombinase under the control of the mouse albumin enhancer/promoter excises the floxed stop cassette and enables expression of *Idh1*^{R132C}. **(B)** Concentration of (R)-2HG in liver from mice at 11 weeks with the indicated genotypes detected by colorimetric (R)-2HG assay. (C: N=3; *CKI*^{R132H}: N = 2; *CKI*^{R132C}: N = 5; N represents mouse numbers) Data represents mean ± SD. ***P < 0.001; unpaired t-test. **(C)** Oncoprint analysis of IDH1 mutant ICCs in the AACR project GENIE 9.0-public dataset, showing concurrent oncogenic genomic alterations in RTK-RAS-MEK pathway genes. **(D and E)** Kaplan-Meier analysis of tumor-free (D) and of overall survival (E). Tumor-free survival was determined as time until tumor progression necessitated euthanasia and included ICC- and HCC-bearing mice. (C: N = 263; CK: N = 125; *CKI*^{R132H}: N = 18; *CKI*^{R132C}: N = 108; N represents mouse numbers). Kaplan-Meier curves were analyzed by log-rank test. ***P < 0.001 was considered statistically significant comparing C and *CKI*^{R132C}. **(F)** Sites of metastatic dissemination observed in the *CKI*^{R132C} GEM model. All metastatic lesions showed ICC histology. **(G)** The table of tumor incidence, latency, and histological phenotype. (†) Percentage of mice in which the particular histology predominates (see Methods). (‡) Percentage of mice in which the particular histology is present in any proportion.



Supplementary Figure S2. Characterization of mIDH1-expressing mouse models

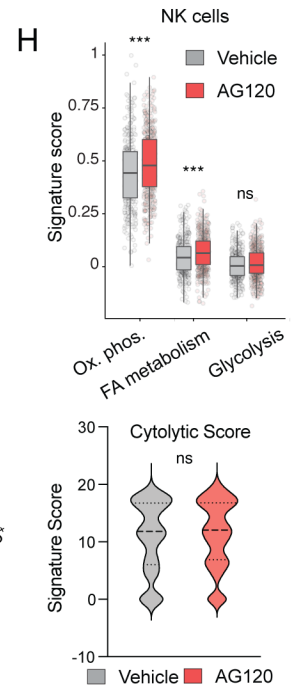
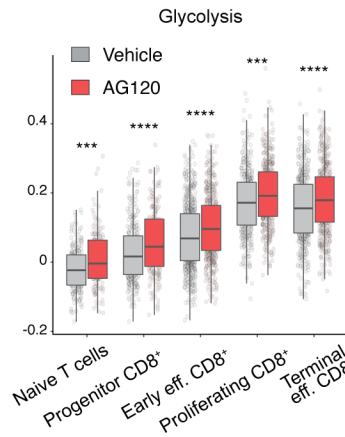
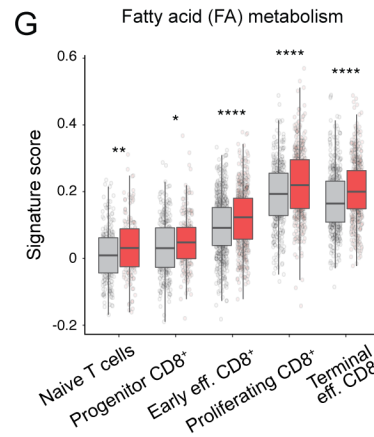
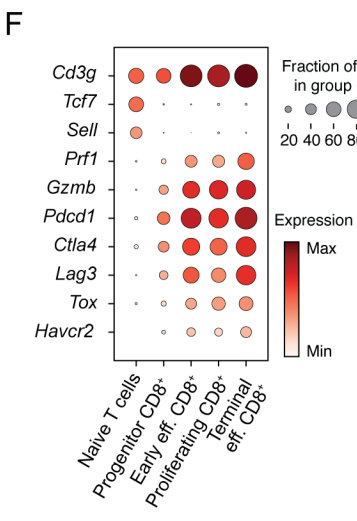
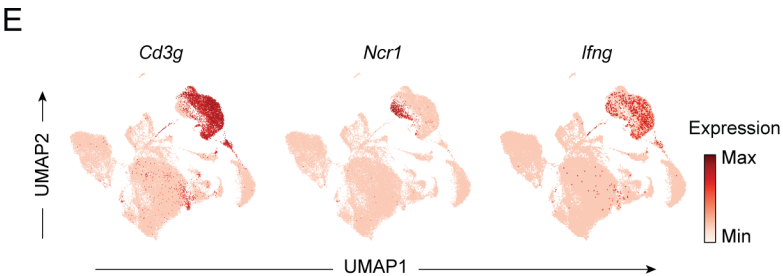
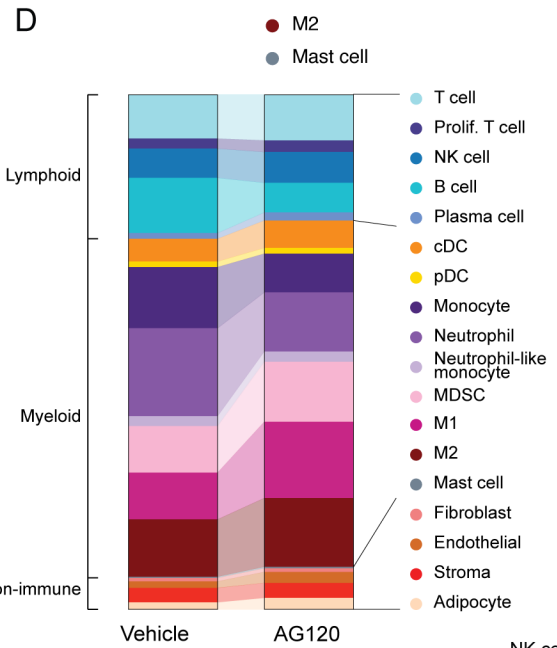
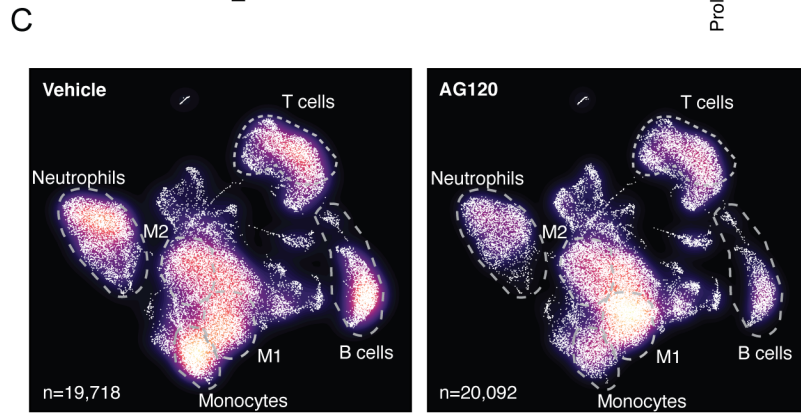
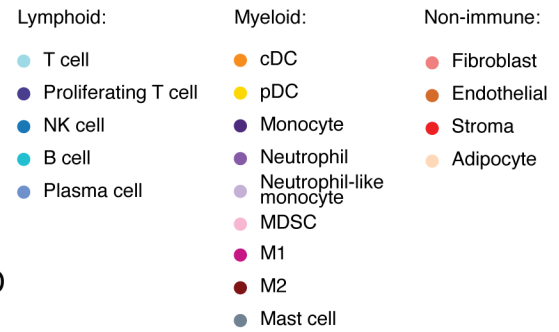
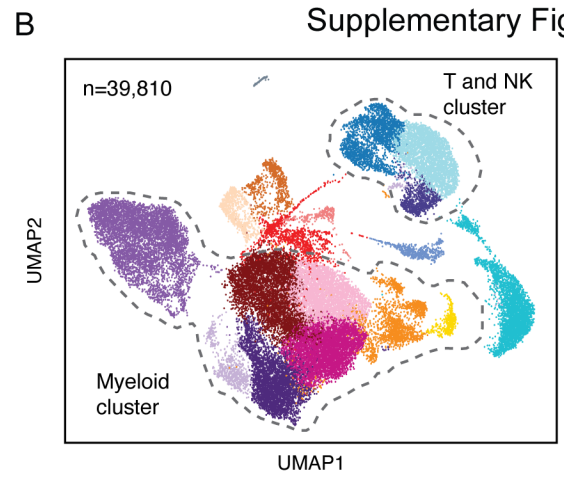
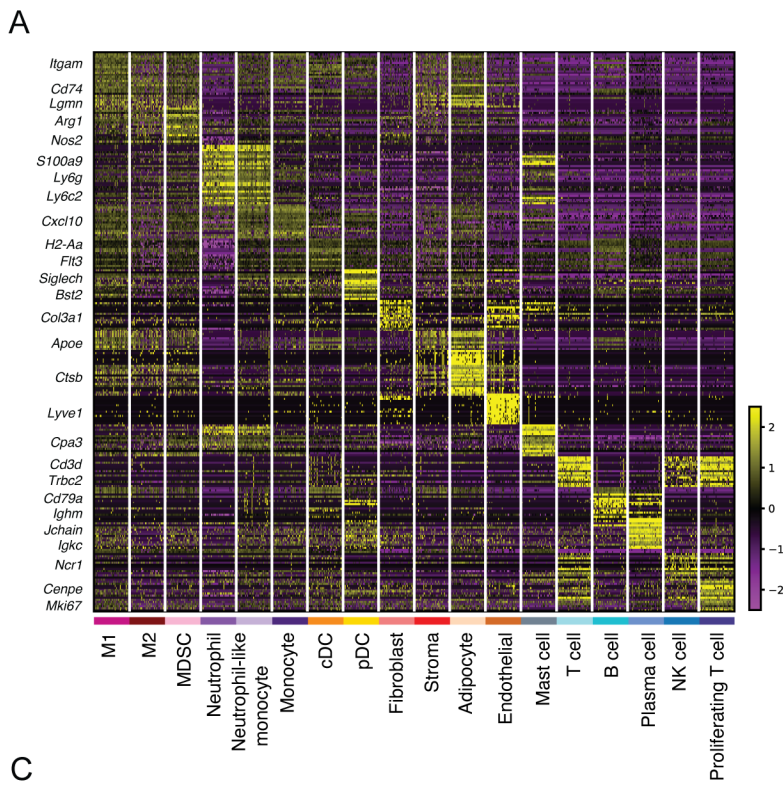
(A, B) Representative H&E-stained section of HCC or ICC from mice of the indicated genotypes (right: higher magnification). **(C)** Tissue sections of ICC and adjacent normal liver from a representative CK1^{R132C} mouse subjected to H&E staining (left panels) and IHC staining against Cytokeratin 19 (CK19) (middle panels) and Alpha-fetoprotein (AFP) (right panels). **(D)** Representative H&E-stained section of livers from mice of the indicated genotypes at 35 weeks. Scale bars: 200 μm (10X panels), 50 μm (40X panels), 100 μm (C).



Supplementary Figure S3. Establishment of allograft models of $Idh1^{R132C}$ ICC

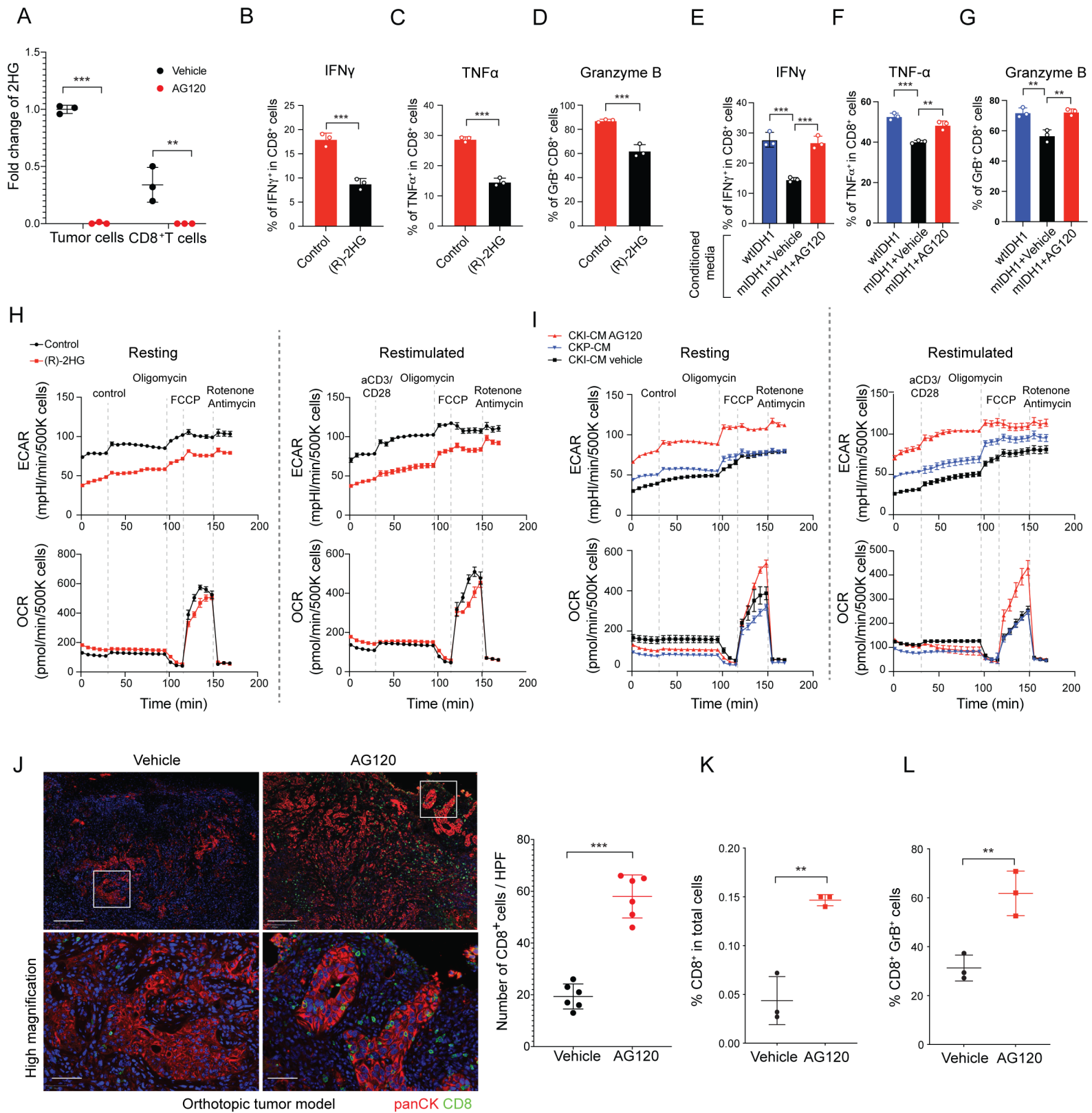
(A) Confirmation of ICC phenotype of tumor cell lines from CKI^{R132C} GEMM via assessment of the relative mRNA expression of the indicated biliary markers. Positive control: ICC cell lines from the murine CKP model (158, 215). Negative controls: murine HCC cell line (Mst1/Mst2 [Stk3/Stk4] KO model) and normal mouse liver. Fold changes were normalized to expression in normal mouse liver. Data represent mean \pm SD. **(B)** Relative concentration of 2HG in CKP (215), CKI^{R132C} (2275-4, 4411 and 2205) primary cell lines detected by GC-MS. Data represent mean \pm SD. **(C)** Relative cell viability in CKI^{R132C} primary cell lines treated with vehicle or 1 μ M AG120. Data represent mean \pm SD. ns=not significant; unpaired t-test. **(D)** Relative concentration of 2HG in CKI^{R132C} primary cell lines treated with vehicle or 1 μ M AG120, detected by GC-MS. Data represent mean \pm SD. *** $P < 0.001$; unpaired t-test. **(E and F)** AG120 *in vivo* kinetics and distribution in plasma (E) and tumor (F). Time course and distribution of AG120 in allograft tumor mouse model using LC-MS/MS (N=3 per timepoint; N represents mouse numbers). **(G and H)** Concentration of (R)-2HG in plasma (G) and in tumor (H) *in vivo* in allograft tumor mouse model using LC-MS/MS. (vehicle: N=4; AG120: N=3 per timepoint; N represents mouse numbers) **(I)** Concentration of AG120 in plasma 12 hours after administration of the last dose, measured by LC-MS/MS. Data represent mean \pm SD. *** $P < 0.001$; unpaired t-test. **(J)** LC-MS/MS measurement of relative level of (R)-2HG in plasma collected 12 hours after the last dose of the 4-day treatment. Data represents mean \pm SD. * $P < 0.05$; unpaired t-test. **(K)** LC-MS/MS measurement of relative level of (R)-2HG in ICCs collected 12 hours after the last dose of the 30-day treatment. Data represents mean \pm SD. * $P < 0.05$; unpaired t-test. **(L)** LC-MS/MS measurement of relative level of (R)-2HG in plasma collected 12 hours after the last dose of the 30-day treatment. Data represents mean \pm SD. * $P < 0.05$; unpaired t-test. **(M)** Immunocompetent wildtype mice were injected subcutaneously with a CKI^{R132C} primary cell line (2275-4). When tumors reached ~ 100 mm³ in volume, animals were randomized into AG120 and vehicle conditions and analyzed for serial

changes in tumor volume. $N = 10$ mice per group. Data represent mean \pm SEM. *** $P < 0.001$; unpaired t-test. **(N)** IHC staining for cleaved Caspase 3 in allograft tumors from mice treated with vehicle or AG120 for 21 days; right: quantification. Data represent mean \pm SD; *** $P < 0.001$; * $P < 0.05$; unpaired t-test. **(O)** Immunocompetent wildtype mice were injected subcutaneously with a CKP primary cell line (254). When tumors reached $\sim 100 \text{ mm}^3$ in volume, animals were randomized into AG120 and vehicle conditions and analyzed for serial changes in tumor volume. $N = 10$ mice per group. Data represent means \pm SEM. *** $P < 0.001$; unpaired t-test. **(P-R)** Immunocompetent wildtype mice were injected orthotopically with a CKI^{R132C} primary cell line. Ten days after engraftment, animals were randomized into AG120 and vehicle conditions and treated for 10 days. **(P)** IHC stained sections for CK19 are shown. The samples were analyzed for changes in tumor area. $N = 3$ mice per group. Data represent mean \pm SEM. *** $P < 0.001$; unpaired t-test. **(Q)** Representative immunofluorescence-stained sections; green: panCK, red: ki67; right: quantification. Data represents mean \pm SD. *** $P < 0.001$; unpaired t-test. **(R)** IHC staining for cleaved Caspase 3; right: quantification. Data represent mean \pm SD; *** $P < 0.001$; * $P < 0.05$; unpaired t-test. **(S and T)** GSEA plots comparing RNA-sequencing profiles of malignant cells (isolated by magnetic bead-mediated depletion of stromal populations) from subcutaneous allograft tumors from immunocompetent mice treated with AG120 and vehicle for 6 days. Genes on the far left (red) correlated the most with upregulated genes by AG120, and genes on the far right (blue) correlated the upregulated genes by vehicle. GSEA was performed with HSIAO_LIVER_SPECIFIC_GENES (panel M) from the C2 (curated gene sets) database in MSigDB and Targets of HNF4 α (panel N) from the TRANSFAC Predicted Transcription Factor Targets database. The vertical black lines indicate the position of each of the genes of the studied gene set in the ordered, non-redundant data set. The green curve corresponds to the ES (enrichment score) curve obtained from GSEA software. Scale bars: 500 μm (M), 50 μm (K; N; O).



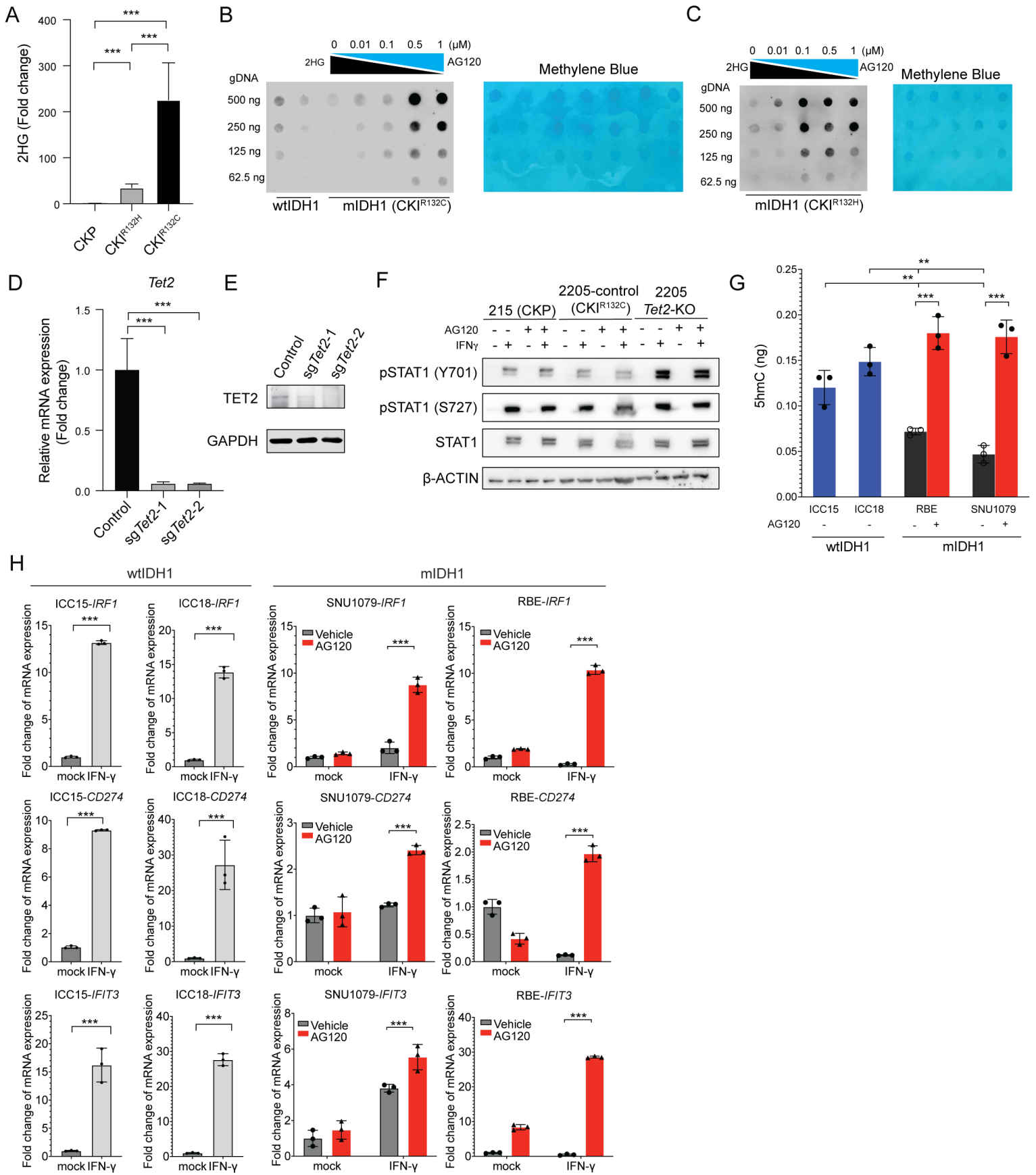
Supplementary Figure S4. Single-cell RNA-seq analysis of the tumor immune microenvironment of mIDH1 ICCs

(A) Heat map of the top genes expressed in each cluster. The columns correspond to the cells; the rows correspond to the genes. Cells are grouped by clusters. The color scale is based on a z-score distribution from -2 (purple) to 2 (yellow). **(B and C)** Identification of tumor-infiltrating immune cell populations. Uniform manifold approximation and projection (UMAP) embeddings of single-cell RNA-seq profiles CD45⁺ leukocyte cells. Representative of one experiment, pooled vehicle-treated (n=4) and AG120-treated mice in orthotopic tumor model. **(D)** Bar plot depicting proportional differences in leukocyte infiltrate from vehicle- versus AG120-treated tumors. Each class contains the following clusters from stroma cells, dendritic cells, pro-immune myeloid, immunosuppressive myeloid, neutrophils and lymphoid. **(E)** Feature plots demonstrating expression of cluster-specific genes: *Cd3g* as a T cell marker, *Ncr1* as a marker of nature killer cells and *Ifng*. **(F)** Dot plot demonstrating the expression of lineage specific genes differentially expressed in different CD8⁺ T cell populations. **(G)** Fatty acid and glycolysis gene signatures score in different CD8⁺ T cells populations. ****<0.0001, ***P<0.001, **P<0.01, *P<0.05. **(H)** Signature scores of oxidative phosphorylation, fatty acid (FA) metabolism, glycolysis (upper) and cytolytic score (lower) in NK cell population.



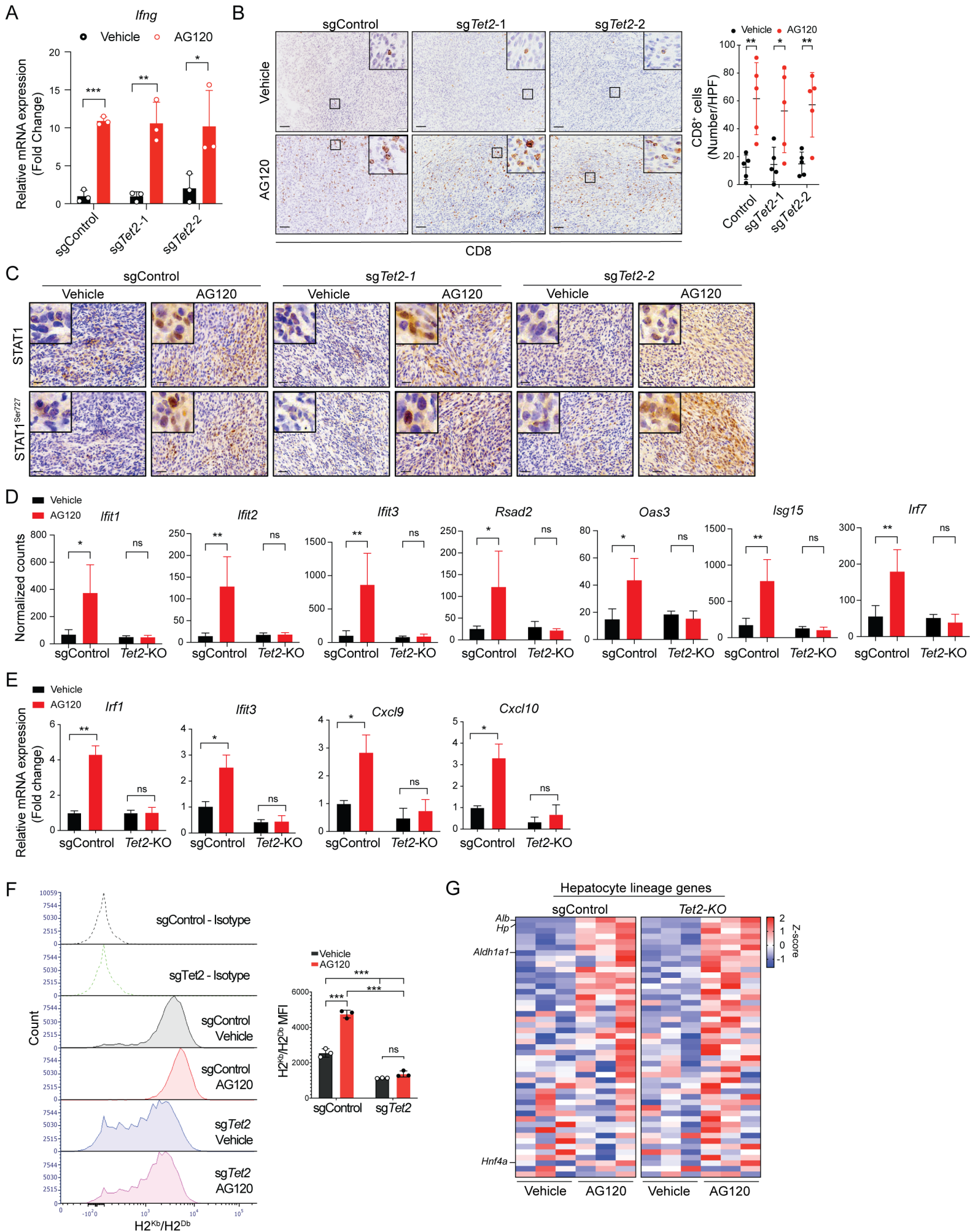
Supplementary Figure S5. Therapeutic efficacy of mIDH1 inhibition in ICC requires CD8⁺ T cell

(A) Relative 2HG in sorted allograft tumors and CD8⁺ T cells with the indicated genotypes detected by GC-MS. ($N = 3$; N represents mouse numbers). Data represents mean \pm SD; ** $P < 0.01$, *** $P < 0.001$; unpaired t-test. **(B-D)** Murine CD8⁺ T cells were activated and rested and then restimulated in the presence of exogenous (R)-2-HG or vehicle for 48 hrs. The graphs show flow cytometry analysis of the percentage of (B) IFN- γ ⁺, (C) TNF α ⁺ and (D) Granzyme B⁺ cells. Data represents mean \pm SD; *** $P < 0.001$; unpaired t-test. **(E-G)** Percentage of (E) IFN- γ ⁺, (F) TNF α ⁺ and (G) Granzyme B⁺ cells in re-stimulated murine CD8⁺ T cells cultured in conditioned media from an IDH WT ICC cell line (CKP) or an mIDH1 ICC cell lines treated with AG120 or vehicle. Data represents mean \pm SD; ** $P < 0.01$, *** $P < 0.001$; unpaired t-test. **(H, I)** Real-time mitochondrial respiration of resting murine CD8⁺ T cells pretreated with either exogenous 30 mM (R)-2HG (H, red color coded) or with conditioned medium from vehicle- (black) or AG120-treated (red) CKI^{R132C} ICC cells (I) for 48 hours and re-stimulated with anti-CD3/CD28 antibody coated beads (aCD3/CD28) (Left panel: resting; right panel: re-stimulated). CD8 T cells treated with conditioned medium from CKP was used as control (I, blue color coded). OCR, oxygen consumption rate; ECAR, extracellular acidification rate; mpH, millipH. Mean \pm s.e.m. **(J)** Study of CD8⁺ T cell infiltrate in orthotopic allograft CKI^{R132C} ICC model after 6 days treatment with vehicle or AG120. Upper: low magnification; Lower: high magnification of fluorescence-stained sections: green: CD8, red: panCK, blue: DAPI; right: quantification. Data represents mean \pm SD; *** $P < 0.001$; unpaired t-test. **(K, L)** Flow cytometry analysis of vehicle- and AG120-treated allograft tumors quantifying (K) CD8⁺ tumor-infiltrating lymphocytes (TILs) among total cells and (L) Granzyme B⁺ cells among CD8⁺ TILs. Data represents mean \pm SD; ** $P < 0.01$; unpaired t-test.



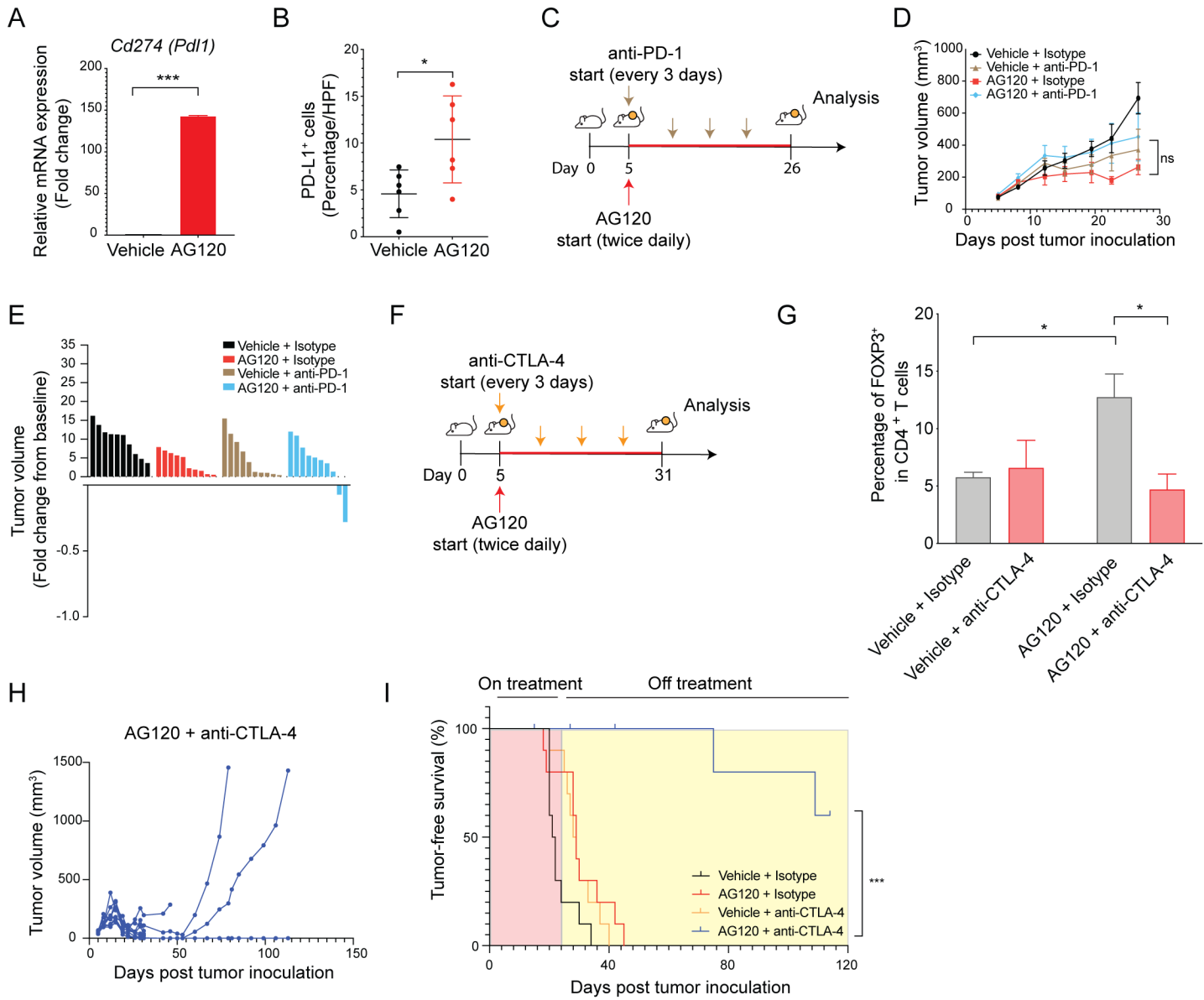
Supplementary Figure S6. IDH1 suppresses 5hmC and IFN- γ response in tumor cells

(A) Relative 2HG in allograft tumors with the indicated genotypes detected by GC-MS. ($N = 3$; N represents mouse numbers). **(B and C)** Dot blot analysis using 5hmC-specific antibodies to detect global levels of 5hmC in two-fold dilutions of genomic DNA from ICC cell lines of the indicated genotypes. CKI^{R132C} (B) and CKI^{R132H} cells (C) were treated serial concentrations of AG120. wtIDH1 cells serve as a control. Methylene Blue staining serves as loading control. **(D and E)** CKI^{R132C} ICC cells were CRISPR-engineered with control sgRNA, sg*Tet2-1* or sg*Tet2-2*. (D) qRT-PCR analysis showing relative *Tet2* mRNA expression. Data represents mean \pm SD. (E) Detection of TET2 protein by immunoblot. GAPDH serves as an internal loading control. **(F)** Immunoblot analysis for levels of phospho-STAT1 (Y701), phospho-STAT1 (S727) and total STAT1 protein in CKP (215), CKI^{R132C}-sgControl (2205-control), and CKI^{R132C}- sg*Tet2* (2205-*Tet2*-KO) ICC cells grown \pm IFN- γ and \pm AG120. β -ACTIN serves as a loading control. **(G)** Bar graphs showing quantification of 5hmC in 400 ng genomic DNA from human wildtype (ICC15 and ICC18) and mutant (RBE and SNU1079) IDH1 choangiocarcinoma cell lines \pm IFN- γ and \pm AG120 detected by ELISA. Data represents mean \pm SD; ** $P < 0.01$, *** $P < 0.001$; unpaired t-test. **(H)** Relative mRNA expression of *IRF*, *CD274*, *IFIT3* in human wildtype (ICC15 and ICC18) and mutant (SNU1079 and RBE) IDH1 choangiocarcinoma cell lines \pm IFN- γ and \pm AG120. mRNA expression was analyzed by real-time RT-PCR using primers that are specific to mouse genes. All data were normalized to *Actb* (mouse) or *ACTB* (human) then to geometric mean of vehicle-treated tumors. Data represents mean \pm SD. *** $P < 0.001$; unpaired t-test.



Supplementary Figure S7. miDH1 suppresses IFN- γ response in tumor cells via TET2 inactivation

(A) Relative mRNA expression of *Ifng* at 15 days of treatment. All data were normalized to *Actb* then to geometric mean of vehicle-treated tumors. Data represent mean \pm SD. *P < 0.05, **P < 0.01, ***P < 0.001; unpaired t-test. **(B)** IHC staining for CD8 at 15 days of treatment; right: quantification. Data represents mean \pm SD; ***P < 0.001; *P < 0.05; unpaired t-test. **(C)** IHC staining for cleaved p-STAT1^{Ser727} in the indicated CRISPR-engineered derivatives of CK1^{R132C} ICC cells grown \pm AG120 *in vivo* for 15 days. **(D)** Bar graphs showing normalized counts of mRNA expression of *Ifit1*, *Ifit2*, *Ifit3*, *Rsad2*, *Oas3*, *Isg15* and *Irf7* enriched in magnetic bead-sorted tumor cells from mice injected with control or *Tet2*-KO CK1^{R132C} ICC primary cell lines treated with AG120 or vehicle for 5 days analyzed using the nCounter PanCancer Mouse Immune Profiling gene expression platform (NanoString Technologies). **(E)** Relative mRNA expression of *Irf1*, *Ifit3*, *Cxcl9* and *Cxcl10* in control and *Tet2*-KO CK1^{R132C} ICC allografts treated or untreated with AG120 or vehicle for 15 days. mRNA expression was analyzed by two-step real-time RT-PCR using primers that are specific to mouse genes. All data were normalized to *Actb* then to geometric mean of vehicle-treated tumors. Data represents mean \pm SD. *P < 0.05, ns: not significant; unpaired t-test. **(F)** Flow cytometry analysis of cell surface expression of H2^{Db}/H2^{Kb} on sgControl and sg*Tet2* miDH1 ICC cells treated with IFN- γ *in vitro*. (Right) Quantification of median fluorescence intensity (MFI) of H2^{Db}/H2^{Kb} of the flow cytometry data. Data represent means \pm SD. ***P < 0.001, ns: not significant; unpaired t-test. **(G)** Heatmap of the differentially expressed hepatocyte lineage genes enriched in magnetic bead-sorted tumor cells from mice injected with control or *Tet2*-KO CK1^{R132C} ICC primary cell lines treated with AG120 or vehicle for 5 days. The analysis was performed using a customized hepatocyte signature panel on the nCounter platform.



Supplementary Figure S8. mIDH1 inhibition synergizes with anti-CTLA4 antibody treatment

(A) Relative mRNA expression of *Cd274* in vehicle- and AG120-treated bulk tumors. mRNA expression was analyzed by two-step real-time RT-PCR. All data were normalized to *Actb* then to geometric mean of vehicle-treated tumors. Data represents mean \pm SD; *** $P < 0.001$; unpaired t-test. **(B)** Quantification of IHC data PD-L1 staining in tumors from vehicle-treated mice and AG120-treated mice. Data represents mean \pm SD; * $P < 0.05$; unpaired t-test. **(C)** Approach to studying combined effect of AG120 and anti-PD-1 antibody treatment in the CKI^{R132C} ICC allograft model. **(D, E)** Immunocompetent wildtype mice were injected subcutaneously with the CKI^{R132C} primary ICC cell line (2205). When tumors reached ~ 100 mm³ in volume, animals were randomized into vehicle + isotype antibody, AG120 + isotype, vehicle + anti-CTLA-4 antibody, and AG120 + anti-CTLA-4 antibody groups. **(D)** Analysis of serial changes in tumor volume. $N = 10$ mice per group. Data represent means \pm SEM. ns: not significant; unpaired t-test. **(E)** Waterfall plot of the maximum percentage change in tumor volume from baseline at day 26 after tumor inoculation. **(F)** Approach to studying cooperative impact of combination AG120 + anti-CTLA-4 antibody in CKI^{R132C} ICC allograft tumor models. **(G)** Flow cytometry analysis of vehicle- and AG120-treated allograft tumors quantifying Treg cells (FOXP3⁺ cells) among CD4⁺ T cells in tumors. Data represents mean \pm SD; * $P < 0.05$; unpaired t-test. **(H)** Serial changes in the volume of individual tumors from AG120 + anti-CTLA-4 antibody treated mice. $N = 10$ mice; N represents mouse numbers. **(I)** Kaplan-Meier analysis for time until tumor progression necessitated euthanasia ($N=10$; N represents mouse numbers). Kaplan-Meier curves were analyzed by log-rank test. *** $P < 0.001$ was considered statistically significant.